Towards a generalized energy prediction model for machine tools

Raunak Bhinge[a], Jinkyoo Park[b], Kincho H. Law[b], David A. Dornfeld[a], Moneer Helu[c] and Sudarsan Rachuri[c]

[a]Laboratory for Manufacturing and Sustainability, University of California, Berkeley, CA, USA
[b]Engineering Informatics Group, Stanford University, Stanford, CA, USA
[c]Systems Integration Division, National Institute of Standards and Technology, Gaithersburg, MD, USA

Abstract

Energy prediction of machine tools can deliver many advantages to a manufacturing enterprise, ranging from energy-efficient process planning to machine tool monitoring. Physics-based energy prediction models have been proposed in the past to understand the energy usage pattern of a machine tool. However, uncertainties in both the machine and the operating environment make it difficult to reliably predict the energy consumption of the target machine. Taking advantage of the opportunity of collecting extensive contextual energy consumption data, this paper discusses a data-driven approach to develop an energy prediction model of a machine tool. First, a data collecting and processing methodology that can efficiently and effectively extract data from a machine tool and its sensors is discussed. We then present a data-driven energy prediction model that can be used to predict the energy consumption of the machine tool for machining a generic part. Specifically, the Gaussian Process (GP) Regression, a non-parametric machine learning technique, is employed in this study for developing the energy prediction model. The energy prediction model is then generalized over multiple process parameters and operations. We finally apply this prediction model to a Mori Seiki NVD1500 machine tool to produce energy consumption predictions with high-level confidence through uncertainty quantification. The methodology can be used to predict the energy consumption for machining any generic part on the same machine with confidence limits. Furthermore, the energy prediction model can be employed to select optimal energy efficient machining strategies and to reduce energy consumption in a machining process.

Email:
Raunak Bhinge : raunakbh@berkeley.edu
Jinkyoo Park : jkpark11@stanfrd.edu
Kincho H. Law : law@stanfrod.edu
David A. Dornfeld : dornfeld@berkeley.edu
Moneer Helu : moneer.helu@nist.gov
Sudarsan Rachuri : sudarsan.rachuri@nist.gov

1. INTRODUCTION

Over 22% of emissions in the US come from the industrial sector, which is also the highest consumer of electrical power in the US (EIA, 2014). Overall, energy consumption by US industries has been declining due to more efficient machine tools and process planning, but the industrial sector continues to be a major energy consumer in the US economy (EIA, 2014). To improve energy use in the manufacturing sector, manufacturers need advanced machine-tool monitoring and operation strategies. Such strategies can enable the development of energy prediction models to estimate electricity costs and peak power demand based on a production plan, which can help manufacturers respond to new regulations and business drivers, such as Smart Grid and carbon cap-and-trade. Energy prediction models can also improve process monitoring since deviations in the power demand and energy consumption of a machine tool can identify different events and states, such as component wear, tool breakage, or collisions (Gutowski, 2006, Vijayaraghavan, 2010). The first step towards achieving advanced machine-tool monitoring and operation strategies is to understand the energy consumption pattern of machine tools and manufacturing operations. In this paper, we use the data collected from a machine tool to determine how different operational strategies influence the energy consumption pattern of a machine tool and to derive an optimal strategy to select efficient operations for machining a part.

Energy prediction models for predicting energy consumption and optimizing manufacturing processes have been a subject of research interest for over 50 years. Most of these efforts are physics-based, i.e., the models are built upon energy patterns and transfer mechanisms of manufacturing operations. Based on the energy transfer from a electrical system to a mechanical system, Neugebauer et al. (2007) formulated a mechatronic representation for computing the total energy consumption of a metal-cutting machine tool. Using energy conservation, Dietmair and Verl (2009) categorized energy consumption of a metal-cutting machine tool by its basic operations, namely the moving axes and material removal, and derived their energy consumption pattern. Although these methods are derived from the basic working principle of a machine tool, they are difficult to implement for practical applications. The methods often require a large number of physical parameters, such as efficiencies of energy transfer between the machine components and the coefficient of friction, which are often hard to compute or estimate. It is often also difficult to properly incorporate the stochastic nature of a manufacturing process into a physics-based model. These difficulties challenge the construction of physics-based models that account for different mechanical characteristics of different machine tools.

Characterizing the energy consumption of a machine tool through experimental data has also been explored. Draganescu et al. (2003) investigated the influence of machining parameters, such as the feed rate, spindle speed, and depth of cut, on the energy consumption of a milling machine tool and constructed statistical regression models using experimental data. Diaz et al. (2009) studied the effect of material removal rate on energy consumption using experimental data and showed that the material removal rate is one key indicator of energy consumption in a machine tool. The work was limited to face-milling operations involving a small set of parameters. Gutowski et al. (2006) developed machine-tool characterization techniques by studying the effects of different process parameters on the total energy consumption. The work gave an understanding of the effects of different parameters on energy consumption in machining. These applications have been limited to specific machining operations, parameter spaces, and tool-workpiece material combinations, which may be insufficient for machine tools with a larger ratio of power demand for material removal to tare power (i.e., power consumption for non-cutting operations and auxiliary equipment). Most of the limitations were due to a limited access to data, lack of standardized data-collection systems, and inefficient data-condensation and post-processing techniques.

Advances in machine automation and sensing technologies now allow continuous measurements of the operating conditions and energy consumption patterns of a machine tool. Such advances provide new opportunities to build data-driven models to characterize a machine tool. Teti et al. (2010) gave an extensive survey of sensor technologies, signal processing, and decision-making methodologies for machine-tool monitoring. MTConnect, an XML-based standard, has been developed to facilitate archiving, accessing and retrieving operational data from various manufacturing equipment (MTConnect Institute,

2014, Vijayaraghavan et al. 2008). MTConnect enables aggregations of raw power data and machining operational information, which provides a means to track variations in energy consumption by different machining operations (Vijayaraghavan and Dornfeld, 2010). MTConnect has been employed to study the effects of different machining process parameters on the energy consumption of a machine tool for producing a part and to construct statistical regression model for energy consumption (Diaz et al., 2011). Although these studies have clearly illustrated the possibility of collecting real-time operational and energy data for future data analysis, they have so far dealt primarily with data collected from slotting operations. In practice, machining a part requires a variety of machine operations with many different combinations of operational parameters. In this study, a generalized energy prediction model is constructed directly from the different machining operations and the combination of the different operational parameters.

Taking advantage of the opportunity to collect extensive energy consumption data, this paper first describes a data processing methodology that efficiently and effectively extracts data from a machine tool controller and add-on sensors. Energy consumption data from an automated milling machine tool (Mori Seiki NVD1500DCG) are collected using MTConnect, which allows us to collect the total energy consumption for producing a part and for every Numerical Control (NC) code block. This allows us to contextualize energy consumption data with the corresponding machining operation and the set of machining operational (control) parameters. To explore all possible combinations of machining parameters for different machining operations, we collect data from 18-machined parts with different machining strategies (NC codes). Utilizing the capability of autonomous data collection using MTConnect, this study then proposes a methodology to construct a generalized data-driven energy prediction model that can be used to predict the energy consumption of the machine tool for machining a generic part. In particular, we apply the Gaussian Process (GP) regression model, a non-parametric regression model, to model the complex input and output relationship. We illustrate the use of the energy prediction model for the evaluation of an optimal strategy for machining a generic part.

2. DATA COLLECTION AND POST-PROCESSING

The first step to construct an accurate energy prediction model of a machine tool is to collect and process data from the target machine. If the machining operational parameters (input) are collected from a wide range of operations and the corresponding measured energy consumption data contains minimum noise, a reliable energy production model can be constructed from these input and output data. However, collecting such extensive data from manually controlled experiments requires significant time and effort, which has been one key barrier for constructing data-driven energy prediction models. Due to recent advancements in sensing and data management, the energy consumption corresponding to each NC code block and its corresponding machining parameters can be collected in real time and efficiently processed and retrieved remotely by the end users. This section discusses how the raw sensor data were collected using MTConnect and how the raw data were processed so that the relevant data could be obtained to construct a data-driven energy prediction model. To demonstrate these data collection and processing procedures, we designed experiments to collect data, including the machine parameters and corresponding energy consumption.

2.1 Data acquisition system

Figure 1 shows the overall data acquisition system used to collect energy consumption data contextualized with machining parameters. The machining data, such as process parameters, NC blocks, and tool positions, were collected from a FANUC controller, and the power time series data was collected using a High Speed Power Meter (HSPM) from System Insights. The machining parameters and the power time series were synchronized and organized using a MTConnect agent. Bhinge et al (2014) and Helu et al. (2014) describe the hardware platform and data acquisition system in greater detail.

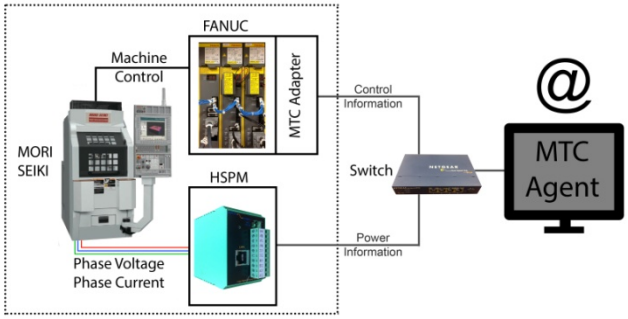

Figure 1. Data acquisition system

2.2 Data processing

Raw data collected using MTConnect is in the form of a time series for both the machining parameters and the energy consumption output. To extract insights about the machine tool, the data collected from a target machine needs to be properly processed and contextualized. When constructing the energy prediction model, the machining process parameters that possibly influence the energy consumption should be extracted from the raw data through a process called feature extraction. Figure 2 shows how the data collected from the target machine may be classified based on the level of post processing applied into three groups: direct, derived, and simulated data.

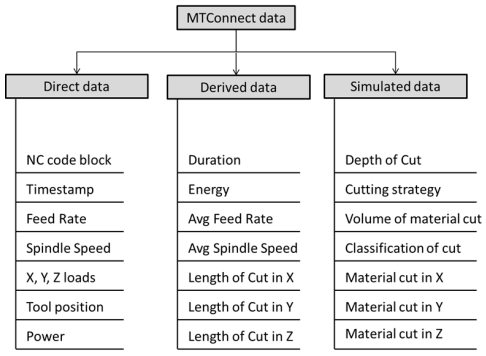

Figure 2. Categorization of types of manufacturing data as obtained using MTConnect

Direct data was the raw data collected from the machine tool controller and added sensors using MTConnect, which included the NC code block, timestamp, instantaneous feed rate, instantaneous spindle speed, instantaneous loads on each axis, instantaneous tool position, and instantaneous power measured using an externally installed power meter. The MTConnect agent synchronized the monitored data using a common time stamp.

Derived data corresponded to cutting operations and was generated by applying simple calculations to sets of direct data. For example, the machining process in conventional automated machine tools is composed of sequences of cutting operations that can be described using a set of machining control parameters represented by an NC code block. To construct the energy prediction model, the relationship between the machining control parameters and the corresponding energy consumption in every NC code bock was studied. Specifically, we computed the total energy, average feed rate, average spindle speed, and length of cut in x- and y-directions over the duration of a block of NC code corresponding to a single cutting operation. We then used the length of cuts in the x- and the y-direction to determine the length and direction of the cut. A sequence of cuts constituted the cutting process of a toolpath .

Simulated data consisted of data generated by simulating the cutting process using direct and derived data. The block-averaged data in each NC code block did not provide enough detail about all possible machining situations. Not every tool movement involved the actual removal of material from the workpiece. For

example, the tool could have moved above the workpiece to position itself for a cut. To determine the actual amount of material removed, we applied a reverse simulation of the entire cutting process, i.e., simulation of the entire cutting process from the instantaneous position data retrieved as direct data. The cutting simulation required prior knowledge of the workpiece dimensions and the tool diameter. To simulate the cutting operation, we constructed a 2-dimensional mesh on the surface of the workpiece, tracked the elements removed during each cut, and redefined the elements in the mesh after every block of NC code. From the positional displacement obtained in the derived data, the toolpath of the tool for each NC code block was tracked and the material removed was calculated. The data extracted from this simulation included the depth of cut, volume of material removed, cutting strategy, and classification of the cut (e.g., air cutting, rapid motion without cutting, feed with cutting). The cutting strategy, i.e., climb or conventional milling, was determined from the cutting simulation by tracking the direction of angular rotation of the tool and the number of elements being cut on either side of the centerline of the tool.

2.3 Experimental design

Energy consumption data corresponding to each block of the NC code and its corresponding machining parameters can be collected in near real time and efficiently processed and retrieved remotely. This motivated a design of experiments to collect data that can realistically represent the manufacturing process by a machine tool. The experimental design and data processing technique used for generating the training data for this study have been described in previous work (Helu, et al., 2014; Bhinge et al., 2014; Park et al., 2015). In this section, we briefly present the basic setup and data processing steps used in the experiments. Figure 3 shows the sample part designed to collect training data for the data-driven energy prediction model. Table 1 shows the specific details of the workpiece, machine tool, and cutting tool used in this experimental study.

As shown in Figure 3, there are five basic cutting operations – face milling, contouring, pocketing, slotting, and plunge – that were involved in machining a part. In addition, there were three non-cutting (i.e., no material removal) operations – air cuts in the $x-y$ and z directions and rapid motion – that were also included in the datasets collected from the experiments. Because process parameters, such as feed rate, spindle speed, and depth of cut, could have affected energy consumption, the test parts were produced using different combinations of machine parameters to investigate the relationship between machining process parameters and energy usage. A Taguchi technique (Box et al., 1979) was employed to design the experiments to ensure a fractional-factorial combination for each set of process parameters in each operation. Table 2 shows the levels chosen for the depth of cut, chip load (feed or thickness of chip removed by one cutting edge of the tool), and spindle speed used to machine the parts. The levels were chosen to cover the entire range of prescribed milling parameters for the tool-workpiece material combination. The feed rate f (mm/min) is the product of the spindle speed (RPM), the number of tool teeth, and the chip load (mm/tooth).

18 parts were machined for this study to provide a total of 196 face-milling, 108 contouring, 54 slotting and pocketing, and 32 plunge experiments. Each line of NC code corresponded to a cutting operation and tool motion and was combined with the corresponding process parameters and output energy consumption. Unlike traditional data collection procedures, each line of NC code for a part was an experiment, i.e., set of process parameters and tool motion features. This allowed us to conduct a large number of experiments by machining a modest number of parts. The face milling operations on the first 9 parts were carried out in the y direction, and the remaining 9 parts were milled in the x direction. The separation of milling operations in the x- and y-directions was necessary to measure the energy consumption accurately for the target machine. The datasets collected from machining all 18 parts were then used to construct the energy prediction model for each (cutting or non-cutting) operation.

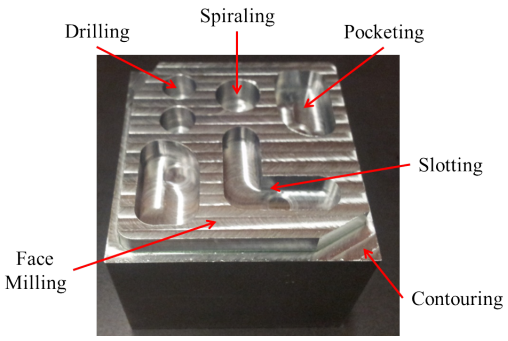

Figure 3. Test part design for experimentation.

Table 1. Experiment details (Bhinge et al., 2014).

Workpiece Material	Cold Finish Mild Steel 1018
Workpiece Dimensions	63.5mm x 63.5mm square cut to a length of 56mm
Machine Make	Mori Seiki NVD 1500
Machine Type	Micro NC Milling Machine
Tool Material	Solid Carbide
Tool Diameter	3/8" (9.525 mm)

Table 2. Experiment levels chosen for different factors.

Level	Spindle Speed (RPM)	Chip Load (mm/tooth)	Depth of Cut (mm)
1	1500	0.0254	1
2	3000	0.0330	1.5
3	4500	0.0432	3
4	6000	0.0508	-

2.4 Data used for energy prediction model

The direct, derived, and simulated data obtained using MTConnect and simulation were used to construct the energy prediction model of the milling machine. There were five basic input (predictor) variables based on the fundamental parameters of a milling machine tool that affect energy consumption (see Figure 4): feed rate, spindle speed, depth of cut, cutting direction, and cutting strategy. Three of the input variables – feed rate, spindle speed and depth of cut – were quantifiable measurements defined as follows:

- $x_1 \in \mathbb{R}$ **Feed rate**: The average velocity at which the tool is fed, which can be retrieved from the controller data
- $x_2 \in \mathbb{R}$ **Spindle speed**: The average rotational speed of the tool, which can be retrieved from the controller data
- $x_3 \in \mathbb{R}$ **Depth of cut**: The actual depth of material that the tool is cutting, which can be obtained from the cutting simulation

The remaining input variables – cutting direction and cutting strategy – were qualitatively (or categorically) labeled. Qualitative variables were represented numerically by codes to construct a regression model. For example, a qualitative variable with K independent categorical features can be represented by a vector of K binary or bits; only a single bit is nonzero to indicate the associated category among K possible categories (Hastie et al. 2009). This approach was used to represent the cutting direction and strategy as coded variables to convert qualitative features into quantitative features:

- $(x_4, x_5, x_6, x_7) \in \{(1,0,0,0), (0,1,0,0), (0,0,1,0), (0,0,0,1)\}$ **Cutting directions**: The indication of the tool's moving direction, which was determined by the lengths of cut in the x-, y-, and z-directions. In

this study, experiments involved only the cutting directions of x-cut, y-cut, z-cut and xy-cut, which were represented as coded variables (1,0,0,0), (0,1,0,0), (0,0,1,0) and (0,0,0,1), respectively.

- $(x_8, x_9, x_{10}) \in \{(1,0,0), (0,1,0), (0,0,1)\}$ **Cutting strategies**: Obtained from the cutting simulation, the cutting strategy was either conventional or climb milling or a combination of both (as in slotting), which were represented as coded variables,(1,0,0), (0,1,0) and (0,0,1), respectively.

Using categorical or coded variables, the prediction model was able to represent any combination of cutting direction and cutting strategy. Furthermore, the use of coded variables allowed the prediction model to be constructed using the entire training data. Otherwise, if an individual prediction function was to be constructed for each combination of cutting direction and cutting strategy, the dataset would have needed to be partitioned into subsets with few data points according to the combination of features.

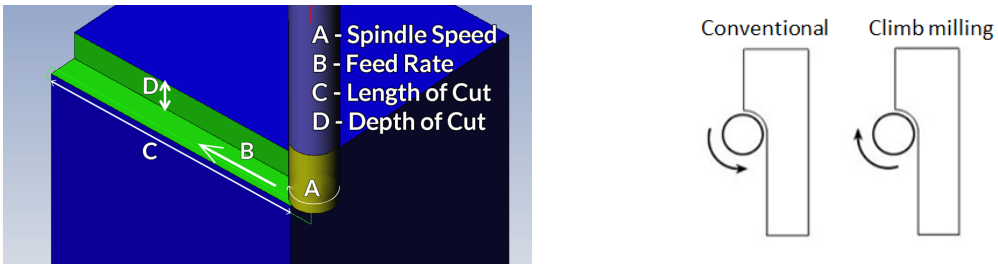

(a) Process parameters of a milling process (b) Cutting strategy

Figure 4. Machining process parameters.

The output (response) variable of the energy prediction model was the energy per unit length of cut, which is a quantitative measure. Within each code block i, the power consumption, $P_k^{(i)}$, $k = 1, \dots, N_P$, over a time duration of t_k, was retrieved as a time series dataset using MTConnect. The total energy consumption, $E^{(i)}$ for NC code block i, was computed as:

$$E^{(i)} = \sum_{k=1}^{N_P} P_k^{(i)} \times t_k. \tag{1}$$

The number of data points, N_P, in each NC code block i depended on the duration of the corresponding operation and the sampling rate for the power measurement, which was 100 Hz in this study. We generalized the energy consumption by using energy density $y^{(i)} = E^{(i)}/l^{(i)}$ (i.e., the energy per unit length of cut) as the output response feature. That is the length of cut scales the predicted energy consumption. Predicting the energy per unit length of cut, or energy density, implicitly included the dependence of the duration of cut on the feed rate and length of cut and allowed us to predict the energy consumption of a part with different (unseen) dimensions, which made the model spatially scalable. Note that we modeled the relationship between the averaged values of the process parameters and the average power (or energy density) across the duration of the block.

For the 18 parts machined for the experiments in this study, a total of 12,299 datasets of input feature vector $\boldsymbol{x}$ and output feature y were generated after post-processing and cutting simulation; each dataset corresponded to an individual NC code block. We filtered out those datasets that corresponded to NC code blocks that had a duration longer than 2 seconds except for rapid motion. This process prevented statistically low quality data from biasing the prediction model since data from blocks of longer duration are more stable. The filtered dataset $\boldsymbol{D} = \{(\boldsymbol{x}^i, y^i) | i = 1, \dots, m\}$, where $m = 3{,}214$ (i.e., data from 3,214 NC code blocks remained after filtering) was further categorized into seven different datasets $\{\boldsymbol{D}_1, \dots, \boldsymbol{D}_q, \dots, \boldsymbol{D}_7\}$ that corresponded to the seven cutting operations described in Figure 3 and Section 2.3; each dataset $\boldsymbol{D}_q = \{(\boldsymbol{x}^i, y^i) | i = 1, \dots, m_q\}$ contained m_q NC code blocks for the cutting operation type q.

3. DATA-DRIVEN APPROACH FOR ENERGY PREDICTION

To construct a data-driven energy prediction model for a machine tool using the data described in Section 2, we can apply Gaussian Process (GP) regression because it can construct a non-linear regression model with high dimensional input features using a relatively small number of training data. As a non-parametric regression technique, GP regression models the input and output relationship without using a set of pre-defined basis functions. Instead, it uses bases formed from the training data. Due to this flexibility, GP regression is able to model complex relationships among input variables and a target response with the least number of hyper-parameters. Additional benefits of GP regression are its ability to quantify uncertainties in the predicted values and its ability to update the regression model incrementally. GP regression has been applied to many fields, including modeling robotics (Nguyen-Tuong et al. 2009), human motions (Wang et al., 2008), and traffic flow (Kim et al. 2011). The following sections describe the procedure we applied to construct the energy prediction model using GP regression.

3.1 Gaussian Process

To construct the energy prediction model for the machine tool, GP regression is employed to approximate the unknown energy prediction function $f(\boldsymbol{x})$ using historical data on the machining process parameters and corresponding energy consumption. A GP is a collection of random variables (stochastic process), any finite set of which has a joint Gaussian distribution (Rasmussen and Williams 2006). By treating the values of the unknown function $f(\cdot) = \mathrm{GP}(m(\cdot), k(\cdot,\cdot))$ as a collection of random variables, GP describes the function probabilistically as a multivariate Gaussian distribution specified by its mean function $m(\cdot)$ and the covariance function $k(\cdot,\cdot)$. The mean function $m(\cdot)$ captures the prior mean of the target function, which is usually assumed to be zero. The covariance function $k(\cdot,\cdot)$ quantifies the correlation between input data in terms of their function values.

In GP regression, we assume that the output $y = f(\boldsymbol{x}) + \epsilon$ is measured with noise $\epsilon \sim N(0, \sigma_\epsilon^2)$, which is Gaussian distributed with zero mean and variance σ_ϵ^2. The values for the unknown function $f(\boldsymbol{x})$ are treated as random variables and modeled by a Gaussian distribution for incorporating prior knowledge captured in the historical data. Suppose the current dataset is denoted by $\boldsymbol{D}_q = \{(\boldsymbol{x}^i, y^i) | i = 1, \dots, m_q\}$ for the machining operation type q. The measured output $y^{new} = f_q(\boldsymbol{x}^{new}) + \epsilon^{new}$ corresponding to the new input feature $\boldsymbol{x}^{new}$ and the historical outputs $\boldsymbol{y}^{1:m_q} = \{y^1, \dots, y^{m_q}\}^T$ in the training dataset $\boldsymbol{D}_q$ follow a multivariate Gaussian distribution (Rasmussen and Williams 2006):

$$\begin{bmatrix} \boldsymbol{y}^{1:m_q} \\ y^{new} \end{bmatrix} \sim N\left(\boldsymbol{0}, \begin{bmatrix} \mathbf{K} & \boldsymbol{k} \\ \boldsymbol{k}^T & k(\boldsymbol{x}^{new}, \boldsymbol{x}^{new}) \end{bmatrix}\right), \tag{2}$$

where $\boldsymbol{k}^T = \{k(\boldsymbol{x}^1, \boldsymbol{x}^{new}), \dots, k(\boldsymbol{x}^{m_q}, \boldsymbol{x}^{new})\}$ and $\mathbf{K}$ is the covariance matrix (kernel matrix) whose (i,j)th entry is $\mathbf{K}_{ij} = k(\boldsymbol{x}^i, \boldsymbol{x}^j)$. The value of the covariance function $k(\boldsymbol{x}^i, \boldsymbol{x}^j)$ quantifies the amount the two input feature vectors $\boldsymbol{x}^i$ and $\boldsymbol{x}^j$ change together. Note that the more the two vectors $\boldsymbol{x}^i$ and $\boldsymbol{x}^j$ differ, the closer the value of the covariance approaches zero, which implies that the two input vectors are not correlated in terms of their function values. An effective kernel function can be chosen considering the characteristics of the target function. Noting that energy consumption varies smoothly with the changes in the machining parameters (Diaz et al. 2011), we use a squared exponential kernel function that can effectively describe a continuously varying function. The squared exponential kernel function evaluates the covariance between the two input feature vectors $\boldsymbol{x}^i$ and $\boldsymbol{x}^j$ as (Neal, 1996):

$$k(\boldsymbol{x}^i, \boldsymbol{x}^j) = \sigma_s^2 \exp\left[-\frac{1}{2}\sum_{r=1}^{n}\left(\frac{x_r^i - x_r^j}{\lambda_r}\right)^2\right] + \sigma_\epsilon^2 \delta_{ij}. \tag{3}$$

The kernel function is described by the hyper-parameters $\boldsymbol{\theta} = \{\sigma_s, \sigma_\epsilon, \boldsymbol{\lambda}\}$. The term σ_s^2 is referred to as the signal variance that quantifies the overall magnitude of the covariance value. The term σ_ϵ^2 is referred to as the noise variance that quantifies the level of noise assumed to exist in the observed output response. The Kronecker delta function δ_{ij} serves to selectively specify the noise variance σ_ϵ^2 to the covariance value

$k(\boldsymbol{x}^i, \boldsymbol{x}^j)$; that is, the noise signals adding to different measurements are assumed to be independent and the noise correlation is non-zero only when $i = j$. The vector $\boldsymbol{\lambda} = (\lambda_1, \dots, \lambda_r, \dots \lambda_n)$ is referred to as the characteristic length scales to quantify the relevancy of the input features in $\boldsymbol{x} = (x_1, \dots, x_r, \dots x_n)$ for predicting the response y. Note that we used a total of $n = 10$ input features in this study. A large length scale λ_i indicates weak relevance, while a small length scale λ_i implies strong relevance of the corresponding input feature x_i.

The hyper-parameters $\boldsymbol{\theta} = \{\sigma_s, \sigma_\epsilon, \boldsymbol{\lambda}\}$ are determined by maximizing the log-likelihood of the measurement data. Using the definition of GP in Eq. (2), the log-likelihood function of data $\boldsymbol{D}_q = \{(\boldsymbol{x}^i, y^i) | i = 1, \dots, m_q\}$ can be expressed as (Rasmussen and Williams 2006):

$$L(\boldsymbol{\theta}; \boldsymbol{D}_q) = P(\boldsymbol{y}^{1:m_q} | \boldsymbol{x}^{1:m_q}; \boldsymbol{\theta}) = N(0, \mathbf{K}) = \frac{1}{\sqrt{(2\pi)^{m_q} |\mathbf{K}|}} \exp\left(-(\boldsymbol{y}^{1:m_q})^T \mathbf{K}^{-1} (\boldsymbol{y}^{1:m_q})\right). \tag{4}$$

Note that $\mathbf{K}$ is the covariance matrix whose (i, j) entries are defined as shown in Eq. (3). The optimum hyper-parameters $\boldsymbol{\theta}^* = \{\sigma_s^*, \sigma_\epsilon^*, \boldsymbol{\lambda}^*\}$ are then determined as that maximize the log-likelihood of the training data $\boldsymbol{D}_q$ as (Rasmussen and Williams 2006):

$$\begin{aligned} \boldsymbol{\theta}^* &= \underset{\boldsymbol{\theta}}{\operatorname{argmax}}\, L(\boldsymbol{\theta}; \boldsymbol{D}_q), \\ &= \underset{\boldsymbol{\theta}}{\operatorname{argmax}} -\frac{1}{2} (\boldsymbol{y}^{1:m_q})^T \boldsymbol{K}^{-1} \boldsymbol{y}^{1:m_q} - \frac{1}{2} \log|\boldsymbol{K}| - \frac{m_q}{2} \log 2\pi. \end{aligned} \tag{5}$$

With the gradient $\nabla \log L(\boldsymbol{\theta}; \boldsymbol{D}_q)$ of the log-likelihood function $L(\boldsymbol{\theta}; \boldsymbol{D}_q)$ available, Eq. (5) can be solved using a mathematical optimization algorithm. We use Gaussian Processes for Machine Learning (GPML), a GP package implemented in MATLAB® to optimize the hyper-parameters (Rasmussen and Nickisch 2013).

After the measurement data and the covariance function (hyper-parameters) are updated, GP regression predicts the unknown response y^{new} corresponding to a new input feature vector $\boldsymbol{x}^{new}$ in a probabilistic fashion. Since the distribution conditional on any subset of the data assumed to be Gaussian distributed is also Gaussian, the posterior distribution $p(y^{new} | \boldsymbol{D}_q, \boldsymbol{x}^{new})$ on y^{new} given the historical dataset $\boldsymbol{D}_q = \{(\boldsymbol{x}^i, y^i) | i = 1, \dots, m_q\}$ and the new input feature vector $\boldsymbol{x}^{new}$ can be expressed as a 1-D Gaussian distribution (Rasmussen and Williams 2006):

$$p(y^{new} | \boldsymbol{D}_q, \boldsymbol{x}^{new}) = N\left(y^{new}; \mu(\boldsymbol{x}^{new} | \boldsymbol{D}_q), \sigma^2(\boldsymbol{x}^{new} | \boldsymbol{D}_q)\right). \tag{6}$$

The posterior distribution $p(y^{new} | \boldsymbol{D}_q, \boldsymbol{x}^{new})$ can be described by its mean μ and variance σ^2, which can be expressed, respectively, as (Rasmussen and Williams, 2006):

$$\mu(\boldsymbol{x}^{new} | \boldsymbol{D}_q) = \boldsymbol{k}^T \mathbf{K}^{-1} \boldsymbol{y}^{1:m_q}, \tag{7}$$

$$\sigma(\boldsymbol{x}^{new} | \boldsymbol{D}_q) = \sqrt{k(\boldsymbol{x}^{new}, \boldsymbol{x}^{new}) - \boldsymbol{k}^T \mathbf{K}^{-1} \boldsymbol{k}}\,. \tag{8}$$

That is, we can obtain the mean function $\mu(\boldsymbol{x}^{new} | \boldsymbol{D}_q)$ from the GP regression to predict the most probable energy density $y^{new} = f_q(\boldsymbol{x}^{new}) + \epsilon^{new}$ for a given input feature vector $\boldsymbol{x}^{new}$ and the standard deviation function $\sigma(\boldsymbol{x}^{new} | \boldsymbol{D}_q)$ to quantify the uncertainty in the predicted value of y^{new} at $\boldsymbol{x}^{new}$. The energy consumption per each machining operation is then aggregated to predict the total energy consumption (with some estimated uncertainty bound) for machining a part.

3.2 Estimating test error

The model selection procedure, i.e., selecting the type of basis function and choosing the optimum feature sets, proceeds before fitting a prediction model to the training dataset. For GP regression, once the type of kernel function is specified, the optimum feature selection is implicitly carried out by optimizing the hyper-parameters for the kernel function. For example, the optimized length scales $\boldsymbol{\lambda} = (\lambda_1, \dots, \lambda_r, \dots \lambda_n)$ for the exponential squared function automatically weigh the importance of the corresponding features in predicting the output response; the smaller λ_r implies the larger influence of the corresponding input feature x_r on the output response y. This property of feature weighting, generally known as automatic relevance determination (ARD) (Neal 1996), simplifies the construction of the energy prediction model since all features are being included to construct the energy prediction functions without explicitly conducting the feature selection procedure.

Depending on the machining operation, the parameters in the input feature vector x affected the energy density value y differently. For each machining operation type q with the dataset $\boldsymbol{D}_q = \{(\boldsymbol{x}^i, y^i) | i = 1, \dots, m_q\}$, we constructed the individual energy prediction function for that operation using GP regression. We then estimated (generalization) errors for each prediction function using the holdout cross validation technique (Hastie et al. 2009). Note that here the (generalization) error was estimated to provide insight into how well each individual energy prediction function would perform with unseen test data.

For each machining operation type q with the dataset $\boldsymbol{D}_q = \{(\boldsymbol{x}^i, y^i) | i = 1, \dots, m_q\}$, we trained the model and computed the error rates as follows:

(1) Randomly divided the dataset D_q into the training dataset D_q^{tr} with m_q^{tr} training data points and the test dataset $\boldsymbol{D}_q^{te}$ with m_q^{te} test data points. In this study, we set the ratio $m_q^{tr} : m_q^{te} = 7:3$, which is a common ratio used to estimate the accuracy (i.e., test error) of predictions for supervised learning algorithms (Hastie et al. 2009).
(2) Constructed the energy density prediction function $f_q(x)$ by computing $\mu(\boldsymbol{x}|\boldsymbol{D}_q)$ and $\sigma(\boldsymbol{x}|\boldsymbol{D}_q)$ using the training dataset $\boldsymbol{D}_q^{tr}$.
(3) Predicted the energy densities corresponding to the input features in the test dataset D_q^{te} and computed the error by comparing them to the true energy densities in the test dataset D_q^{te}. The error was measured in terms of the mean absolute error (MAE), which was more insensitive to outliers than the root mean square error (RMSE) (Willmott and Matsuura 2005):

$$\mathrm{MAE}_q = \frac{1}{m_q^{te}} \sum\nolimits_{\{(\boldsymbol{x}^i, y^i) \in \boldsymbol{D}_q^{te}\}} \left| \mu(\boldsymbol{x}^i|\boldsymbol{D}_q) - y^i \right|. \tag{9}$$

MAE_q quantifies how close the predictions were compared to the measured values. To quantify how much the predicted values in terms of a ratio to the mean density $\bar{y}_q$ for the machining operation type q, we use the normalized mean absolute error (NMAE) (Gustafson and Shaocai 2012):

$$\mathrm{NMAE}_q = \frac{\sum_{\{(\boldsymbol{x}^i, y^i) \in D_q^{te}\}} \left| \mu(\boldsymbol{x}^i|\boldsymbol{D}_q) - y^i \right|}{\sum_{\{(\boldsymbol{x}^i, y^i) \in \boldsymbol{D}_q^{te}\}} y^i} = \frac{\mathrm{MAE}_q}{\bar{y}_q}. \tag{10}$$

Note that we could have computed the average deviation between the predicted and measured densities, *i.e.*, MAE_q, by simply multiplying NMAE_q with the measured mean density $\bar{y}_q$ (for the machining operation type q).

The value of NMAE_q could have fluctuated depending on the selected training and test datasets. To quantify the test error reliably, the 100 values of NMAE_q were computed by repeating the above procedure 100 times. The averaged value μ_{NMAE} was then determined and used as an error measure in this study. Note that the number of repetitions is empirically determined to come up with a stable, representative mean value irrespective of the selected training and test datasets.

Table 3 compares the estimated (generalization) errors for the energy density prediction function for each operation type. The machining operations are categorized into three types: feed with cut, air cut, and rapid motion. For feed with cut, the cutting tool is engaged with the workpiece and removing material. For air cut, the cutting tool moves but does not contact the workpiece. For rapid motion, the tool is moving rapidly to reposition itself without contacting the workpiece. The feed with cut operation can be further categorized into face milling, contouring, slotting, pocketing, and plunge depending on how the machine removes the workpiece material. The averages for the normalized mean absolute error μ_{NMAE} (computed using 100 NMAE values from 100 test experiments) for the cutting operations are different due to the different cutting mechanisms as well as the different number of training data used for constructing the models. Overall the μ_{NMAE} values range between 8% and 45% and are smaller for the feed with cut operations. The standard deviation σ_{NMAE} for the average for the normalized mean absolute error quantifies the variability in the estimated μ_{NMAE}. As shown in Table 3, when the number of training data is small, for example in the plunge and rapid motion operations, the estimated value fluctuates significantly. Since the average duration of a rapid motion is extremely small as compared to other operations, the data quality is much lower, which results in a greater prediction error and variation. To gain better insight into the accuracy of the energy prediction model, the value of μ_{NMAE} can be compared to the coefficient of variation (CV) capturing the inherent fluctuation in the energy density values in the training dataset. The coefficient of variation is computed based on absolute difference between the energy densities and its mean:.

$$\text{CV} = \sum_{i=1}^{N} \left| y^i - \bar{y} \right| \Big/ \sum_{i=1}^{N} y^i = 77.165\% \tag{11}$$

The values of μ_{NMAE} obtained by the energy prediction model are much lower than the value of CV, which implies that the energy prediction model captures well the variations in the energy density induced by different machine operations and parameters.

Table 3: The estimated test error for each energy density prediction function (for rapid motion, the time filtering is not applied since the duration of rapid motions are mostly less than 2 sec).

Operation type		Number of NC blocks	Average duration (sec)	$\mu_{\bar{y}_q}$ (J/mm)	μ_{MAE} (J/mm)	μ_{NMAE} (%)	σ_{NMAE} (%)
Feed with cut	Face milling	1225	18.973	221.963	18.736	8.440	0.472
	Contouring	401	7.278	247.463	30.957	12.488	1.585
	Slotting	119	4.753	240.515	26.148	10.881	1.173
	Pocketing	196	4.213	262.518	33.423	12.735	1.935
	Plunge	115	8.461	1722.108	501.457	29.189	3.212
Non cut	Air cut	384	6.999	841.273	70.157	8.350	0.798
	Rapid motion	110	0.528	100.572	44.069	44.653	12.521

3.3 Uncertainty quantification in the prediction model

Using the energy density prediction model for each machining operation type q represented by the mean energy density function $\mu_q(\boldsymbol{x}|\boldsymbol{D}_q)$ and the associated standard deviation function $\sigma_q(\boldsymbol{x}|\boldsymbol{D}_q)$, the total energy consumption for machining a part can be estimated from the NC codes. First, we can estimate the energy consumption $\hat{E}^i$ and the standard deviation S^i from the input feature $\boldsymbol{x}^i$ of the NC code block i performing the machining operation type q as:

$$\hat{E}^i = \mu_q(\boldsymbol{x}^i|\boldsymbol{D}_q) \times l^i, \tag{12}$$

$$S^i = \sigma_q(\boldsymbol{x}^i|\boldsymbol{D}_q) \times l^i, \tag{13}$$

where l^i is the length of cut specified for the operation by the NC code. Aggregating all the NC blocks for the machining operation type q, the predicted total energy consumption $\hat{E}_q$ and the associated standard deviation S_q can be computed for that operation type:

$$\hat{E}_q = \sum_{\{(\boldsymbol{x}^i, y^i) \in \boldsymbol{D}_q\}} \mu_q(\boldsymbol{x}^i | \boldsymbol{D}_q) \times l^i, \tag{14}$$

$$S_q = \sqrt{\sum_{\{(\boldsymbol{x}^i, y^i) \in \boldsymbol{D}_q\}} \left(\sigma_q(\boldsymbol{x}^i | \boldsymbol{D}_q) \times l^i\right)^2}. \tag{15}$$

Finally, the estimated total energy consumption $\hat{E}$ for machining a whole part and the standard deviation S associated with the estimation can be computed by summing the mean predicted energy $\hat{E}_q$ and accumulating the standard deviation S_q for all machining operation types, $q = 1, \ldots, Q$, where $Q = 7$ (including all cutting and non-cutting operations). Because the energy consumed in each machining operation is considered independent of the energy consumed by other machining operations, $\hat{E}$ and S are expressed as:

$$\hat{E} = \sum_{q=1}^{Q} \hat{E}_q, \tag{16}$$

$$S = \sqrt{\sum_{q=1}^{Q} \left(S_q\right)^2}. \tag{17}$$

Note that the energy density $\hat{y}$ is represented to be a Gaussian random variable in the framework of GP regression. Because a linear combination of Gaussian random variables is also Gaussian, the predicted total energy E, which is computed as a linear combination of the energy densities, is also Gaussian. The probability distribution on the total energy E then can be expressed as $E \sim N(\hat{E}, S^2)$ with the mean $\hat{E}$ and the standard deviation S given in Eq. (16) and Eq. (17), respectively.

4. VALIDATION TESTS

The energy prediction model constructed based on GP regression model (as described in Section 3) was used to predict the energy consumption for machining a generic part. This section discusses the validation of the trained energy prediction function using unseen test data.

4.*1 Data collection from a blind test*

Figure 5 shows a generic part, the geometry of which is quite different from the part used in the training process (see Figure 3). The cutting and non-cutting operations used to produce the generic test part are face milling, pocketing, plunge, air cut, and rapid motion.

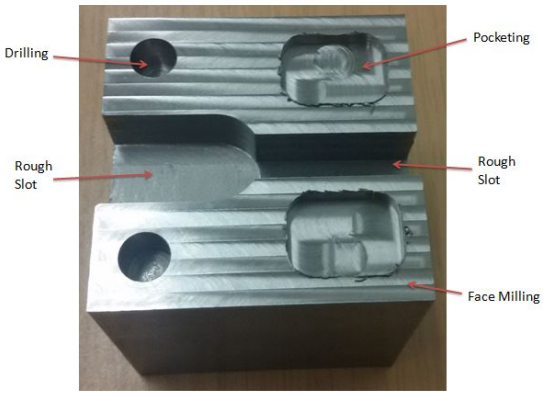

Figure 5. Generic test part used to validate the energy prediction model

The accuracy of the energy prediction model depended on how the machining parameters for a test part were distributed relative to the machining parameters used in the training dataset. If the machining parameters for the test part were completely different from the machining parameters used to collect the training dataset, the accuracy of the prediction fell. To study how the energy prediction model generalized over unobserved test data, we validated the energy prediction model by machining three test parts with the geometry shown in Figure 5, but we intentionally varied the spindle speeds in these experiment as shown in Table 4. Comparing the spindle speeds used to the 18 training parts to those in Table 4, the first test part uses the same spindle speed while the second and third use different spindle speeds from those of the training datasets. We chose these spindle speeds to evaluate the model's capability of predicting the energy density values in incrementally more unexplored parameter space. For all test parts, the depth of cut was set to 1 mm.

Table 4: Spindle speeds chosen for the blind tests

	Used spindle speeds (in RPM)
Training parts 1~18	{1,500; 3,000 4,500}
Test part 1	{1,500; 3,000; 4,500}
Test part 2	{1,700; 2,800; 4,300}
Test part 3	{2,130; 2,400; 3,750}

4.*2 Prediction result*

Figure 6 shows the measured energy density values y and the predicted energy density function $\hat{y}$ for the face milling operations with different spindle speeds and different feed rates. To visualize the high-dimensional prediction function for the energy density, we fix the other machining parameters for y-direction cut and conventional cutting strategy and set the depth of cut to 1 mm. For each plot, the curve shows how the energy density varies with the feed rate for fixed spindle speed. The influence of the spindle speed on the energy density can be studied by comparing the curves shown in the figure. In each plot, the dash line represents the predicted mean $\mu_1(\boldsymbol{x}|D_1)$ and shaded band represents the 95% confidence bound on the predicted energy density, i.e., $\mu_1(\boldsymbol{x}|D_1) \pm 1.96\sigma_1(\boldsymbol{x}|D_1)$.

As Figure 6 shows, the energy density measurements for the face milling operations in test parts 1, 2, and 3 are well captured by the energy density prediction function for each spindle-speed/feed-rate combination. The overall trend of the energy density is well predicted by the mean function $\mu_1(\boldsymbol{x}|D_1)$. In addition, most measurements are within the 95% confidence bound on the predicted energy density. The width of the confidence bound changes depending on the distribution of the training data used to build the model. In general, the confidence bound for high feed rate is larger because a fewer number of data points were collected in this region to build the model.

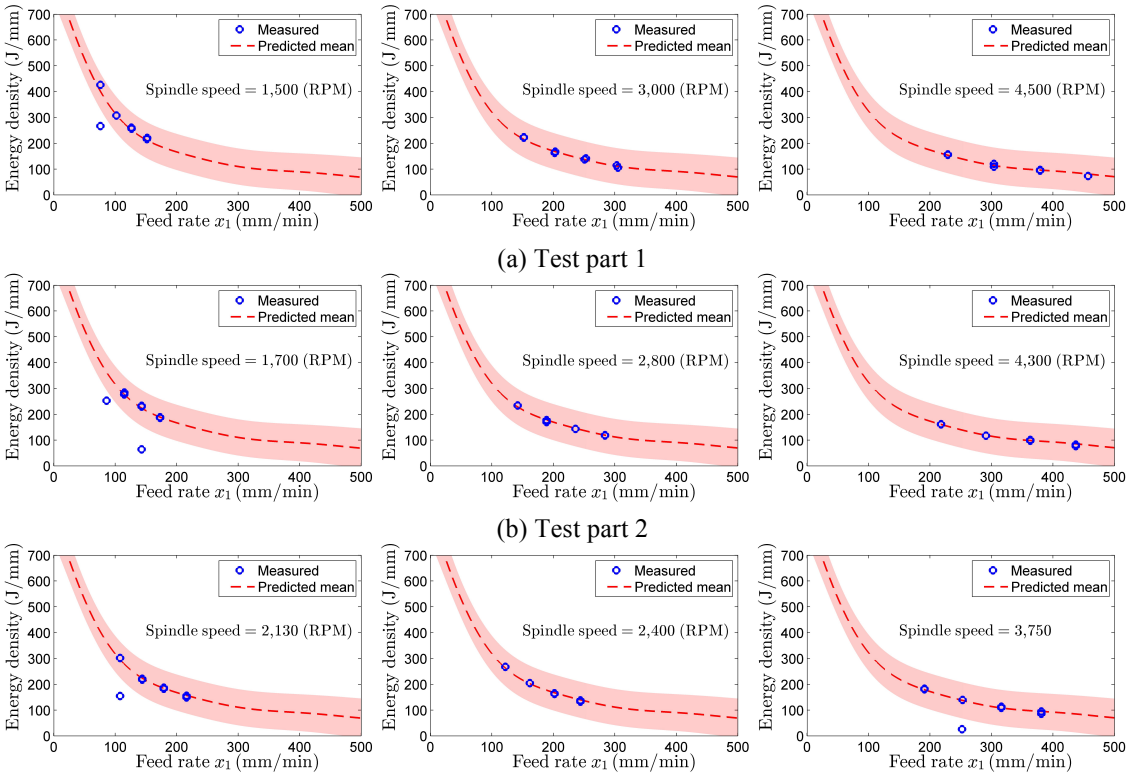

(a) Test part 1

(b) Test part 2

(c) Test part 3

Figure 6. Predication of energy density values for generic test parts (machined using face-milling, y-direction cut, conventional cutting strategy, and depth of cut = 1mm). The band represents $\mu_1(\boldsymbol{x}^i|D_1) \pm 1.96\sigma_1(\boldsymbol{x}^i|D_1)$.

Figure 7 compares the predicted and the measured energy consumption for each individual NC code block. To predict the energy consumption $\hat{E}^i$ for block i, the type of machine operation q is first identified and the energy density prediction function $\mu_q(\boldsymbol{x}^i|\boldsymbol{D}_q)$ corresponding to that operation q is used. The predicted (mean) energy for block i is then computed using Eq. (12). In general, the predicted energy consumption values match well with the measurements. The deviation of the mean energy prediction from the measured energy consumption increases from test part 1 to 3. This is because the machining parameters in test part 3 are the furthest away from the observed values in the training data.

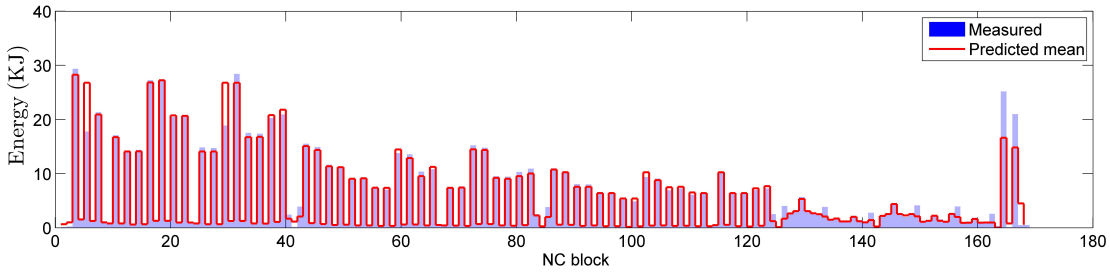

(a) Test Part 1

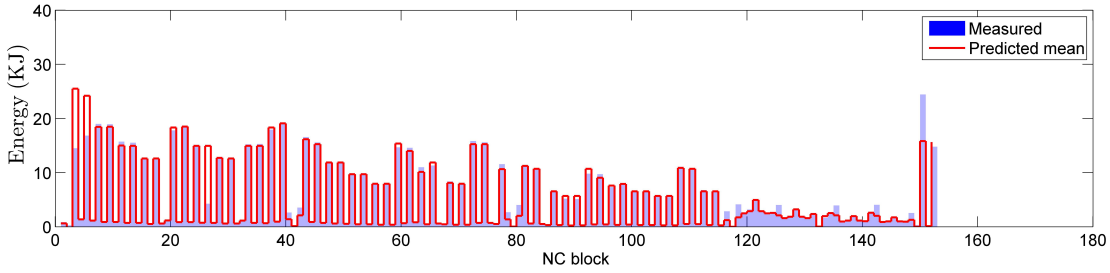

(b) Test Part 2

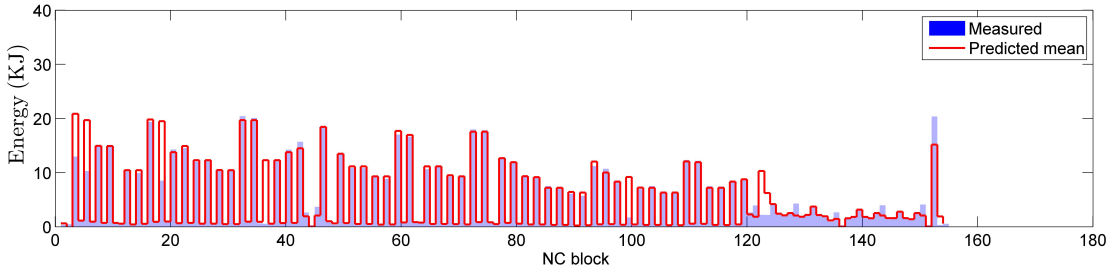

(c) Test Part 3

Figure 7. Predication of total mean energy consumptions including all operations

Finally, Table 5 compares the predicted and measured energy consumption using the normalized mean absolute error (NMAE) and relative total error (RTE) defined as:

$$\text{NMAE} = \frac{\sum_{\{i \in \text{ NC blocks}\}} \left|\hat{E}^i - E^i\right|}{\sum_{\{i \in \text{ NC blocks }\}} E^i}, \tag{18}$$

$$\text{RTE} = \frac{\left|\hat{E} - E\right|}{E}. \tag{19}$$

Note that the NMAE in Eq. (18) is defined using the predicted energy $\hat{E}^i$ and the measured energy E^i for each NC code block i, whereas the NMAE in Eq. (10) is defined using the predicted energy density $\hat{y}^i$ and the measured energy density y^i. Thus, the energy prediction with the longer length of cut l^i will contribute more to the value of NMAE in Eq. (18). In spite of this dependence on the geometry, the measure can still quantify the mean absolute errors of the three test cases in a relative manner. As Table 5 shows, the NMAE for the three test parts are less than 15%, which are consistent with the estimated error using the training dataset based on the hold-out cross-validation method. In other words, the energy prediction model generalizes quite well for the unseen test dataset, which validates the effectiveness of the model in predicting the energy consumed to machine a generic part.

While the NMAE quantifies error in the predicted energy for a single cut, the RTE quantifies the errors in the predicted total energy consumption for producing a whole part. Table 5 shows that for all test cases, the RTE is less than 6%. In addition, the measured total energy falls within the 95% confidence bound $\hat{E} \pm 1.96S$ on the predicted total energy. The RTEs for the energy prediction are small for all three test parts because the errors $\hat{E}^i - E^i$ are distributed centering at the zero-mean with an almost equal chance to over- or underestimate the energy as shown in Figure 8. The overestimations and the underestimations on the block-wise energy consumptions are canceled out when they are summed up to compute the total energy consumption. Therefore, the block wise energy prediction results in accurate estimation on the total energy consumption for machining a whole part.

Table 5: Summary of prediction results on the generic test parts

	No. of data	Averaged block duration (sec)	NMAE (%)	Measured Total energy (KJ)	Prediction total energy (KJ)	Standard deviation (KJ)	RTE (%)
Test 1	168	10.014	9.577	909.266	891.022	35.259	-2.007
Test 2	152	9.567	10.359	768.605	766.901	37.696	-0.222
Test 3	154	9.577	13.553	761.272	806.761	34.508	5.976

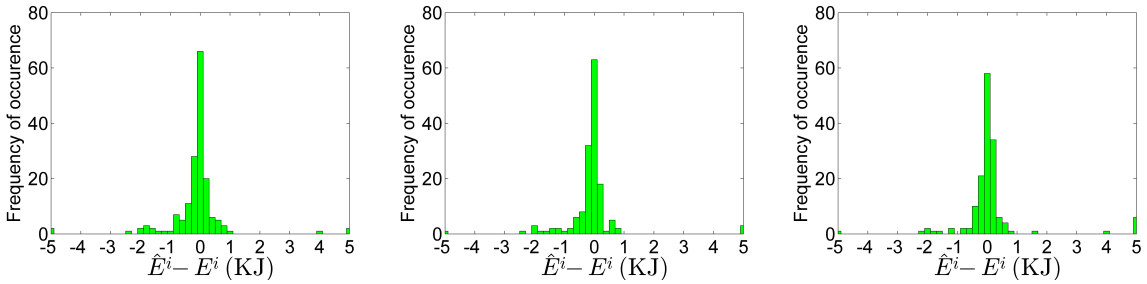

(a) Test part 1 (b) Test part 2 (c) Test part 3

Figure 8. Distributions of errors

5. OPTIMIZING MACHINING STRATEGIES

In addition to predicting the energy consumption, the energy prediction functions can also be used to determine an efficient toolpath to machine a part or to enable novel monitoring strategies by highlighting abnormal behavior. In this section, we discuss the use of energy prediction functions to select the optimum toolpath that uses the least amount of energy to machine a part.

5.*1 Experiments for toolpath planning*

The coordinates (x, y, z) with respect to the global reference represent the location of the cutting tool. The toolpath is then described by the temporal sequences of the machine tool coordinates. The tool's sequential moves with respect to the geometry of a workpiece determine the cutting direction and the cutting strategy, which can possibly affect the energy consumption. Figure 9 shows four different toolpaths that were explored to machine a pocket shown in Figure 10. Table 4 shows the process parameters used to execute these four different toolpaths. Each toolpath is composed of cuts in different directions and with different cutting strategies. The goal is to select the toolpath that minimizes energy consumption before actually machining the part by predicting energy consumption using the energy prediction function. This prediction can then be compared to the true energy consumption measured during experiment.

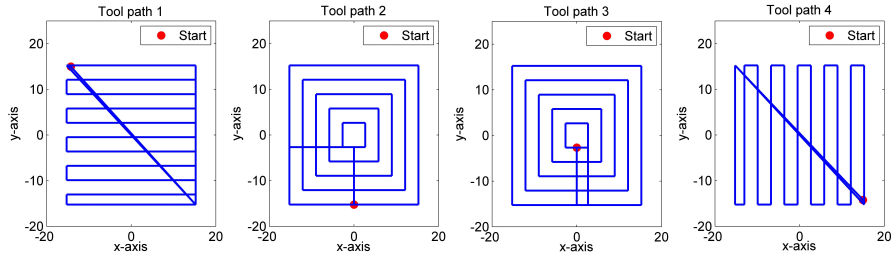

Figure 9. Toolpath comparison

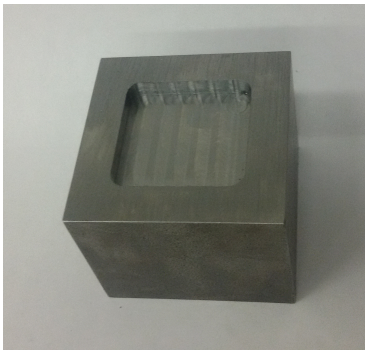

Figure 10. Part geometry for ordering different toolpath strategies

Table. 6. Process parameters used in the experiments to order different toolpaths

Levels	Cutting Speed (RPM)	Chip Load (inches)	Depth of Cut (mm)
1	1500	0.001	1.5
2	300	0.002	1.5

5.*2 Optimum toolpath selection*

Table 7 summarizes the results of the experiments to machine the part shown in Figure 10 using the four different toolpaths in Figure 9. The required energy varies depending on the toolpath used, and the energy prediction function predicts the total energy consumption with good accuracy. Figure 11 compares the measured and predicted energies for each toolpath. The error bar on the predicted energy usage represents the 95% interval, i.e., $\mu \pm 1.96\sigma$, for the predicted total energy consumption. Note that the measured energy values all fall within the 95% confidence bound on the predicted total energy. With the predicted energies, the toolpaths can be ordered in terms of their energy consumption, and the optimum toolpath with the minimum energy consumption can then be selected accordingly.

Table. 7. Summary of prediction results on the toolpath comparison using the generalized energy prediction function.

	No. of data	Averaged block duration (sec)	NMAE (%)	Measured Total energy (kJ)	Prediction total energy (kJ)	Standard deviation (kJ)	RTE (%)
Path 1	73	6.806	11.041	273.389	282.377	9.466	3.288
Path 2	111	5.181	15.436	303.466	320.896	8.995	5.744
Path 3	109	5.415	11.655	327.643	338.277	8.788	3.246
Path 4	84	6.225	16.015	301.907	311.833	11.300	3.288

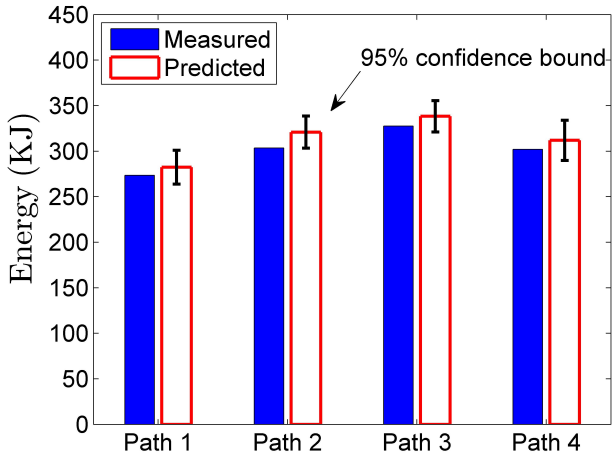

Figure 11. Total energy consumption comparison for different toolpath strategies.

6. CONCLUSIONS

This study demonstrates the use of a non-parametric regression model, namely the Gaussian Process (GP), to predict the energy consumption of a machine tool. The GP models the complex relationship between the input machining parameters and output energy consumption and constructs a prediction function for the energy consumption with confidence bounds. Even though the training datasets in this study include only 18 experimental parts, the models constructed using the machine learning approach are able to reliably predict the energy consumption for machining a generic test part with the milling machine tool. In addition, the energy prediction function is used to select the optimum toolpath that uses the least amount of energy to machine the same part. The prediction models can be updated and, possibly, improved as further experimental datasets are collected. For example, we plan to study the influence of material properties on the energy consumption pattern of a machine tool by generalizing the energy prediction model to embrace different material types.

To effectively establish the energy consumption pattern of a machine tool over time, the energy prediction model would need to be continuously updated with new measurement data to account for the time-varying characteristics of the machine tool due to, e.g., tool wear and machine tool deterioration. Incorporating these characteristics, particularly tool wear, into the modeling approach is one area of future study. Another area of future work is constructing a near-real-time energy prediction model for a machine tool by combining a near-real-time data collection framework and an adaptive GP regression model. We are currently developing a near-real-time data collection framework to retrieve raw data from a milling machine tool and its sensors and convert them into relevant input features. In addition, we are currently investigating the use of sparse representation of the covariance matrix to reduce the computational and storage demands of GP regression, which can help to update the GP regression model with near-real-time streaming data. It is expected that the energy prediction function can be constructed using a fraction of training data points (perhaps as few as 10%), which can reduce the training time without sacrificing accuracy significantly.

As alluded to in Section 5, the energy prediction model that is being continually updated can be used to monitor the conditions of machine components. One area where we can apply energy prediction for machine tool monitoring is anomaly detection, i.e., a sudden, unexpected deviation between the predicted and actual energy consumption value may indicate an abnormal event. For example, if a tool breaks or if a collision occurs (perhaps due to incorrect tool offsets), then the actual energy consumption may be significantly different from the predicted value, which can trigger an immediate alarm. Developing monitoring strategies based on energy prediction represents a potentially impactful area of future study.

In conclusion, this study shows that with advanced data collection and processing techniques, prediction models can be constructed to predict energy consumption of a machine tool with multiple operations and multiple process parameters. The specific energy prediction model that was generated in this study would work for generic parts machined on an NVD1500. The methodology that was described, though, could be used to create prediction models for other machine tools to enable improved planning and operations in various shop-floor environments.

Acknowledgement and Disclaimer

The authors acknowledge the support by the Smart Manufacturing Systems Design and Analysis Program at the National Institute of Standards and Technology (NIST), Grant Numbers 70NANB12H225 and 70NANB12H273 awarded to University of California, Berkeley, and to Stanford University respectively. In addition, the authors appreciate the support of the Machine Tool Technologies Research Foundation (MTTRF) and System Insights for the equipment used in this research. Certain commercial systems are identified in this paper. Such identification does not imply recommendation or endorsement by NIST; nor does it imply that the products identified are necessarily the best available for the purpose. Further, any opinions, findings, conclusions, or recommendations expressed in this material are those of the authors and do not necessarily reflect the views of NIST or any other supporting U.S. government or corporate organizations.

REFERENCE

Bhinge, R., Park, J., Biswas, N., Helu, M., and Dornfeld, D., Law, K., and Rachuri, S. (2014). "An Intelligent Machine Monitoring System Using Gaussian Process Regression for Energy Prediction," *IEEE International Conference on Big Data* (IEEE BigData 2014), Washington, DC.

Box, G., Hunter, J.S., and Hunter, W.G. (1979). "Statistics for Experimenters: Design, Inovation, and Discovery," Wiley.

Diaz, N., Helu, M., Jarvis, A., Tonissen, S., Dornfeld, D. and Schlosser, R. (2009). "Strategies for Minimum Energy Operation for Precision Machining," *Proceeding of MTTRF 2009 Annual Meeting*, Shanghai, China.

Diaz, N., Redelsheimer, E. and Dornfeld, D. (2011). "Energy Consumption Characterization and Reduction Strategies for Milling Machine Too Use," *Proceeding of 18th CIRP International Conference on Life Cycle Engineering,* Braunschweig, Germany.

Dietmair, A. and Verl, A. (2009). "Energy Consumption Forecasting and Application for Tool Machines," *Modern Machinery Science Journal,* pp. 62-67.

Draganescu, F., Gheorghe, M. and Doicin, C.V. (2003). "Models of Machine Tool Efficiency and Specific Consumed Energy," *Journal of Material Processing Technology,* 141, pp. 9-15.

Gustafson, W.I., and Shaocai, Y. (2012). "Generalized Approach for Using Unbiased Symmetric Metrics with Negative Values: Normalized Mean Bias Factor and Normalized Mean Absolute Error Factor," *Atmospheric Science Letter*, 13(4), pp. 262-267.

Gutowski, T., Dahmus, J. and Thiriez, A. (2006). "Electrical energy requirements for manufacturing processes," *Proceedings of 13th CIRP International Conference of Life Cycle Engineering*, Lueven, Switzerland.

Hastie, T., Tibshirani, R. and Friedman, J. (2009). The Elements of Statistical Learning, Springer, New York, NY.

Helu, M., Robinson, S., Bhinge, R., Bänziger, T., and Dornfeld, D. (2014). "Development of a Machine Tool Platform to Support Data Mining and Statistical Modeling of Machining Processes," *Proceeding of*

MTTRF 2014 Annual Meeting, San Francisco, CA

Kim, K., Lee, D. and Essa, I. (2011). "Gaussian Process Regression Flow for Analysis of Motion Trajectories," *Proceeding of IEEE ICCV*.

MTConnect Institute (2014). MTConnect v. 1.3.0, http://www.mtconnect.org/downloads/standard.aspx.

Neal, R. M. (1996). Bayesian learning for neural networks, Springer-Verlag, New York.

Neugebauer, R., Denkena, B. and Wegener, K. (2007). "Mechatronics Systems for Machine Tools," *Annals of the CIRP,* 56, pp. 657-686.

Nguyen-Tuong, D., Seeger, M. and Peters, J. (2009). "Model learning with local Gaussian process regression," *Advanced Robotics,* 23(15), pp. 2015-2034.

Park, J., Bhinge, R., Biswas, N., Srinivasan, M., Helu, M., Rachuri, S., Dornfeld, D. and Law, K. (2015). "A generalized data-driven energy prediction model with uncertainty for a milling machine tool using Gaussian Process," *ASME 2015 International Manufacturing Science and Engineering* Conference, Charlotte, NC

Rasmussen, E and Nickisch, H. (2013). Gaussian process regression and classification toolbox version 3.2, downloaded from: http://www.gaussianprocess.org/gpml/code/matlab/doc/.

Rasmussen, C., and Williams, C. (2006). "Gaussian Process for machine learning," MIT Press.

Teti, R., Jemielniak, K., O'Donnell, G. and Dornfeld, D. (2010). "Advanced monitoring of machine operations," *CIRP Annals-Manufacturing Technology*, 50, pp. 717-739

U.S. Energy Information Administration (EIA). (2014). AEO2014 Early Release Overview, Report Number: DOE/EIA-0383ER.

Vijayaraghavan, A., Sobel, W., Fox, A., Dornfeld, D. and Warndorf, P. (2008). "Improving Machine Tool Interoperability Using Standard Interface Protocols: MTConnect," *Proceeding of 2008 International Symposium on Flexible Automation*, Atlanta, USA.

Vijayaraghavan, A. and Dornfeld, D. (2010). "Automated Energy Monitoring of Machine Tools," *CIRP Annals – Manufacturing Technology*, 59, pp. 21-24.

Wang, J.M., Fleet, D.J and Hertzmann, A. (2008). "Gaussian Process Dynamical Models for Human Motion," *IEEE Transactions on Pattern Analysis and Machine Intelligence*, 30(2), pp. 283–298.

Willmott, C., and Matsuura, K. (2005). "Advantage of the Mean Absoute Error over the Root Mean Square Error (RMSE) in Assessing Average Model Performane," *Climate Research*, 30, pp. 79-82.